Journal of Applied Electrochemistry **34**: 1141–1145, 2004.

Corrosion performance of NiAl intermetallic with Mo, Ga and Fe in neutral and alkaline media

A. ALBITER[1], M.A. ESPINOSA-MEDINA[1], M. CASALES[2] and J.G. GONZALEZ-RODRIGUEZ[3]*
[1]*Instituto Mexicano del Petroleo, Eje Central Lázaro Cárdenas, México, D.F., México*
[2]*U.N.A.M. Centro de Ciencias Físicas, AV. Universidad S/N, Cuernavaca, Mor., México*
[3]*Universidad Autónoma del Estado de Morelos, F.C.Q.I.-C.I.I.C.A.P. Av. Universidad 1001, Col. Chamilpa, 62210-Cuernavaca, Mor., México*
*(*author for correspondence, e-mail: ggonzalez@uaem.mx)*

Received 7 August 2003; accepted in revised form 16 June 2004

Key words: aqueous corrosion, mechanical alloying, nickel aluminides

Abstract

The corrosion resistance of mechanically alloyed NiAl intermetallics with additions of Mo, Ga and Fe, and their combinations, has been studied using potentiodynamic polarization curves and linear polarization resistance tests at room temperature. Solutions included 0.5 M NaCl and 0.5 M NaOH. The Al–42Ni + 6Fe and Al–40Ni + 6Fe + 2Mo alloys exhibited the best corrosion resistance in NaCl whereas the highest corrosion rate was observed on Al–39Ni + 6Fe + 6Mo alloy, above the NiAl-base alloy. In NaOH, the highest corrosion rate was exhibited by Al–41Ni + 6Mo alloy, whereas the best corrosion performance was obtained by alloys with 6Ga, followed by alloys containing 6Fe + 2Ga and/or 2Mo + 2Ga, and NiAl-base alloy had an intermediate corrosion rate. The alloys with the lowest corrosion rate also had the lowest pitting potential values. So, generally speaking, additions of 6Mo decreased the corrosion resistance of NiAl-base alloys in these environments. The results were supplemented by detailed scanning electronic microscopy studies and chemical microanalysis of the corroded specimens.

1. Introduction

Nickel aluminide, NiAl, is an intermetallic compound that forms as a result of the ordering of the nickel and aluminum atoms on the f.c.c. unit cell. As a promising intermetallic, it can be used at low or high temperature due to its high melting point (1638 °C), low density, and excellent thermal conductivity. These characteristics make nickel aluminide a promising candidate as a structural material for both ambient and high temperature applications. Although interest on nickel aluminide is primarily due to its potential for high temperature applications, it also possesses certain properties which make it a possible candidate for low temperature applications. Its corrosion resistance is due to its ability to form a dense, adherent, protective aluminum oxide layer. However, NiAl is too brittle at room temperature and it has poor creep properties in respect to more conventional alloys [1–4]. Major efforts have been centered on enhancing the mechanical properties through grain refinement, micro and macro-alloying as well as ductile phase toughening [5–7]. Also, recent theoretical work has indicated promising results through grain refinements [8]. The incorporation of a second phase has also been reported by improvement in high and low temperature properties [9]. The sintering of nanocrystalline powders performed at low temperatures has been carried out in short times replacing the commercial Ni-base superalloys [10] through the additions of iron (Fe), molybdenum (Mo) and gallium (Ga). The evaluation of NiAl alloy corrosion resistance in aqueous media is interesting. Furthermore, its application at high temperature due to temperature changes in the process may lead to catastrophic failure during service.

The objective of this work is to evaluate the differences in corrosion behavior among NiAl alloys with minor additions of Fe, Ga and Mo in aqueous 0.5 M NaCl and in 0.5 M NaOH at room temperature.

2. Experimental procedure

Materials used were intermetallic NiAl alloys with additions of Mo, Ga and Fe. They were prepared by mechanical alloying the elemental powders under argon atmosphere at room temperature followed by vacuum hot pressing as described elsewhere [10]. Mechanical alloying was carried out in a SPEX 8000D mixer/mill. Ni, Al, Ga, Fe and Mo were 99.99% pure. To perform the corrosion test experiments, specimens of $5 \times 5 \times 3$ mm were machined by an electrodischarge machine,

encapsulated in epoxy resin and then polished with diamond paste to a 0.1 μm finish. Electrochemical experiments were performed using an ACM-Instruments potentiostat controlled by a PC. Potentiodynamic polarization curves were obtained by varying the applied potential from −500 mV with respect to the free corrosion potential, E_{corr}, up to +600 mV at a rate of 1 mV s^{-1}. Before the experiments, the E_{corr} value was measured for approximately 30 min, until it stabilized. All the potentials were measured using a saturated calomel electrode (SCE) as reference. The counterelectrode was graphite. Corrosion rates were calculated in terms of the corrosion current, i_{corr}, by using linear polarization resistance curves, LPR, which was done by polarizing the specimen from −10 to +10 mV, with respect to E_{corr}, at a scan rate of 1 mV s^{-1}, which is a standard scanning rate for this kind of experiment, to get the polarization resistance, R_p. Using the Stearn–Geary [11] equation, the i_{corr} value was calculated as follows:

$$i_{corr} = \frac{b_a b_c}{2.3(b_a + b_c)} \cdot \frac{1}{R_p} \quad (1)$$

where b_a and b_c are the anodic and cathodic slopes obtained from the polarization curves. The corrosion rates, in mm $year^{-1}$, were calculated using Faraday's law. All tests were performed at room temperature (25 ± 2 °C). Solutions used included 0.5 M sodium chloride (NaCl) and 0.5 M sodium hydroxide (NaOH), which were prepared from analytical grade reagents. After the experiments, the specimens were cleaned to be observed in the scanning electronic microscope (SEM) and microchemical analysis of the corroded specimens were done with an energy dispersive X-ray analyzer (EDS) attached to it (Table 1).

3. Results and discussion

Figure 1 shows the effect of Fe, Mo and Ga on the polarization curves of NiAl alloys in 0.5 M NaCl. All the alloys exhibited a passive region. The corrosion potential (E_{corr}) values varied over a wide range; thus, the lowest value was for the NiAl + 2Mo + 2Ga alloy, around −768 mV, whereas the NiAl-base alloy had a value of −385 mV and the highest value, −285 mV, was for the NiAl + 6Mo alloy. The lowest corrosion current densities values, i_{corr} were for the NiAl + 6Fe and NiAl + 6Fe + 2Mo respectively, whereas the highest values were for the base NiAl alloy showing no beneficial effect of the alloying elements. The change in pitting potential (E_{pit}) values was in the same fashion as the E_{corr} values, i.e. the lowest E_{pit} value was for NiAl + 2Mo + 2Ga whereas the highest value was for the NiAl + 6Mo alloy. In contrast, Figure 2 shows that in 0.5 M NaOH solution, the NiAl-base alloy had the lowest i_{corr} value and highest E_{corr} value, showing the beneficial effect of Fe, Mo and Ga in this environment. In 0.5 M NaOH all the alloys also developed a passive region, which means that in NaOH and in NaCl solutions, all the NiAl-base alloys are susceptible to

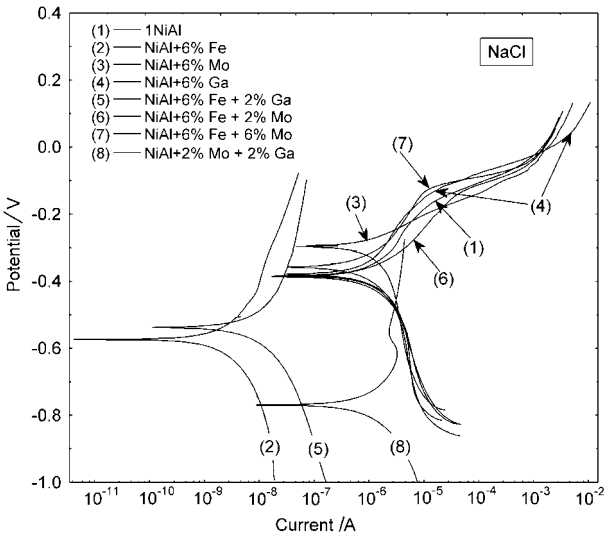

Fig. 1. Polarization curves of NiAl based alloys obtained in 0.5 M NaCl solution.

Table 1. Chemical compositions (at.%) of NiAl alloys with additions of Fe, Ga and Mo

Alloy #	Nominal composition (at.%)	Chemical composition as by EDS (at.%)
1	Al–44Ni	51.76 Al–48.24Ni
2	Al–42Ni + 6Fe	52.57 Al–41.15Ni–6.29Fe
3	Al–41Ni + 6Mo	52.79 Al–40.86Ni–6.35Mo
4	Al–41Ni + 6Ga	52.63 Al–41.25Ni–6.12Ga
5	Al–40Ni + 6Fe + 2Mo	50.99 Al–40.23Ni–6.47Fe–2.31Mo
6	Al–40Ni + 6Fe + 2Ga	51.09 Al–41.05Ni–5.98Fe–1.88Ga
7	Al–39Ni + 6Fe + 6Mo	48.49 Al–39.08Ni–6.28Fe–6.15Mo
8	Al–42Ni + 2Mo + 2Ga	54.25 Al–41.78Ni–1.89Mo–2.08Ga

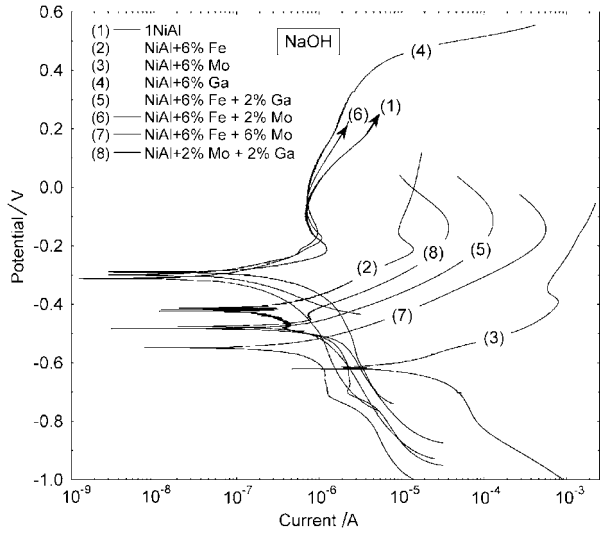

Fig. 2. Polarization curves for NiAl based alloys tested in 0.5 M NaOH solution.

pitting corrosion. However, in 0.5 M NaCl all the alloys exhibited an active–passive behavior, whereas in 0.5 M NaOH, they showed an active–passive–transpassive behavior. The effect of Fe, Mo and Ga on the E_{pit} value was the same as in E_{corr} values. A summary of E_{corr} and i_{corr} values for both environments are given in Table 2.

A change in corrosion rate with time in 0.5 M NaCl for the different NiAl-base intermetallics is given in Figure 3. Generally speaking, the NiAl + 6Mo + 6Fe alloy had the highest corrosion rate, whereas the most corrosion resistant alloy was the one alloyed with 6Fe + 2Mo. The NiAl-base alloy had a relatively low corrosion rate, around 10 times lower than the least resistant, and very similar to the most resistant. Initially the corrosion rate of the NiAl alloy was one of the highest; its corrosion rate decreased with time until it reached a low, steady value for 0.5 M NaCl. This behavior implies that most of the alloying elements had a detrimental effect, leading to an increase in corrosion rate of the base material. The only beneficial alloying elements were a combination of 6Fe + 2Mo.

In 0.5 M NaOH (Figure 4), on the other hand, the NiAl + 6Mo alloy had the highest corrosion rate, and additions of 6Fe + 2Ga or 6Ga decreased the corrosion rate of the base alloy. In the latter case, the corrosion rate was decreased by almost one order of magnitude, whereas the former increased the corrosion rate by two orders of magnitude, showing a very detrimental effect of 6Mo in NaOH, and 6Fe + 6Mo in NaCl. Specimens corroded in 0.5 M NaOH showed deep pits, as shown in Figures 5 and 6, which show the corroded surface of alloys containing 6Fe + 2Mo and 2Mo + 2Ga respectively. X-ray studies on the specimens with the highest corrosion rate, i.e. NiAl + 6Mo, showed that the structure contained mainly the NiAl phase with big Mo_2C precipitates [10] whereas the NiAl-base alloy contained the NiAl and Al_2O_3 phases only. On the other hand, the specimens corroded in 0.5 M NaCl presented hardly any pitting corrosion, as can be seen in Figures 7 and 8. In this case, the alloy with the highest corrosion rate was that alloyed with 6Fe + 6Mo, which also contained the NiAl phase with the Mo_2C precipitates.

Figures 9 and 10 show an EDS analysis of the corrosion products formed on the specimens corroded in 0.5 M NaCl and in 0.5 M NaOH. In sodium chloride, we can see the presence of Al, Ni, Mo Cl and O, as main elements, except for alloy 4, which was only alloyed with Ga, and consequently the peak for Mo is absent. The same happened for tests in sodium hydroxide; the peaks

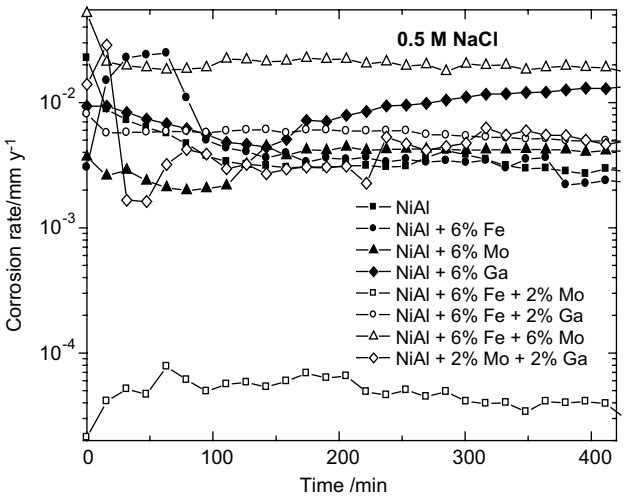

Fig. 3. Effect of Fe, Mo and Ga on the change in corrosion rate for NiAl based alloys in 0.5 M NaCl solution.

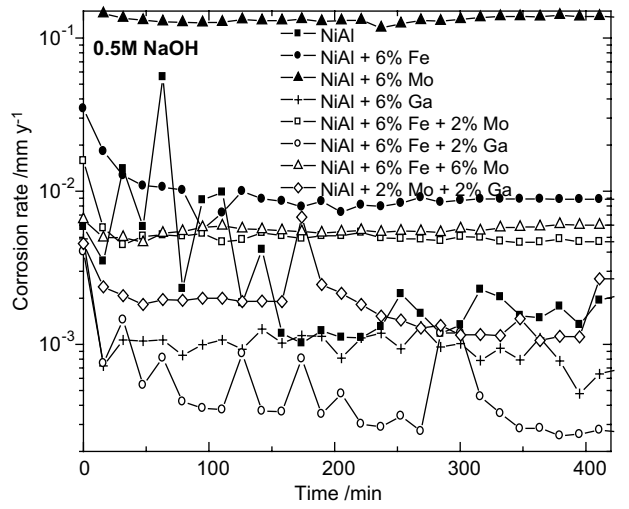

Fig. 4. Effect of Fe, Mo and Ga on the change in corrosion rate for NiAl based alloys in 0.5 M NaOH solution.

Table 2. Summary of the E_{corr} and i_{corr} values obtained from polarization curves for the NiAl-based alloys tested in 0.5 M NaCl and in 0.5 M NaOH solutions

Alloy	0.5 M NaCl		0.5 M NaOH	
	E_{corr} (mV)	i_{corr} (A m^{-2})	E_{corr} (mV)	i_{corr} (A m^{-2})
Al–44Ni	−385	5.0×10^{-7}	−290	2.0×10^{-7}
Al–42Ni + 6Fe	−572	2.0×10^{-9}	−424	2.0×10^{-7}
Al–41Ni + 6Mo	−285	7.0×10^{-7}	−614	7.0×10^{-6}
Al–41Ni + 6Ga	−379	8.0×10^{-7}	−298	2.1×10^{-7}
Al–40Ni + 6Fe + 2Mo	−537	7.0×10^{-9}	−482	5.0×10^{-7}
Al–40Ni + 6Fe + 2Ga	−382	8.0×10^{-7}	−311	6.0×10^{-8}
Al–39Ni + 6Fe + 6Mo	−358	3.4×10^{-6}	−549	4.0×10^{-7}
Al–42Ni + 2Mo + 2Ga	−768	1.0×10^{-6}	−475	2.0×10^{-7}

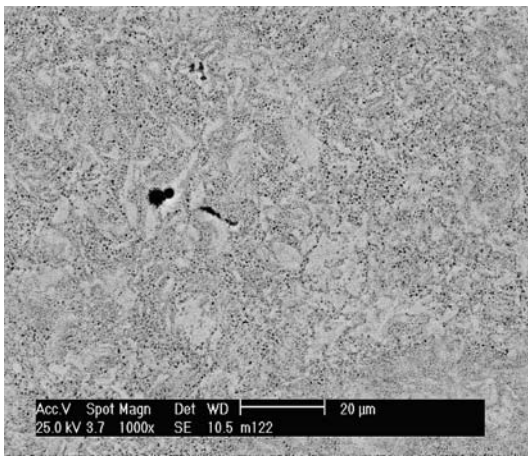

Fig. 5. SEM image of alloy 4 (NiAl + 6Ga) corroded in 0.5 M NaOH solution.

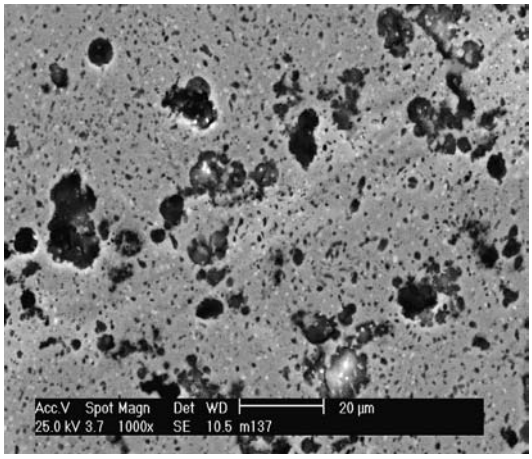

Fig. 6. SEM image of alloy 7 (NiAl + 6Fe + 6Mo) corroded in 0.5 M NaCl solution.

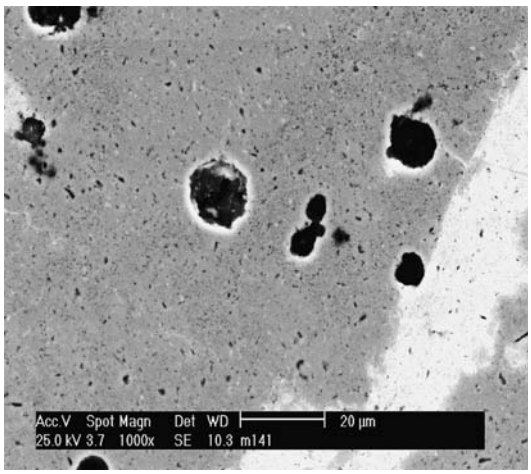

Fig. 7. SEM image of alloy 5 (NiAl + 6Fe + 2Mo) corroded in 0.5 M NaOH solution.

of Ni, Al, Mo and O appear again, although the intensity of the peaks for Ni is lower than in sodium

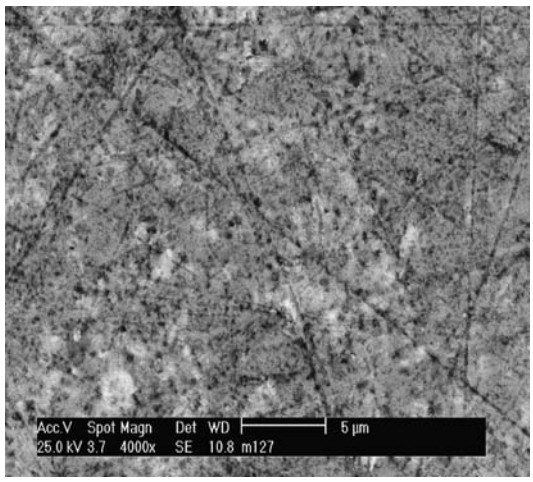

Fig. 8. SEM image of alloy 8 (NiAl + 2Mo + 2Ga) corroded in 0.5 M NaCl solution.

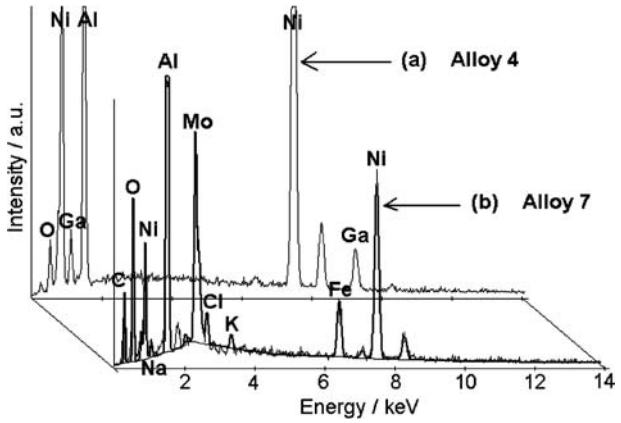

Fig. 9. EDS analysis of the corrosion products for: (a) alloy 4 in NaOH solution and (b) alloy 7 in NaCl solution.

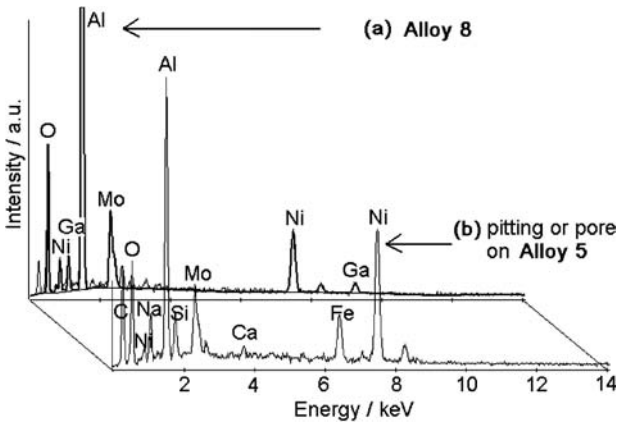

Fig. 10. EDS analysis of the corrosion products for: (a) alloy 8 in NaCl solution and (b) pitting or pore of the alloy 5 in NaOH solution.

chloride. It should be noted that the passive film, usually has several layers. Molybdenum was detected in the outer zone of the passive film, whereas nickel does not enter the passive film [12, 13]. Zhang [14] studied the corrosion of aluminum implanted with Mo in 0.1 M

NaCl and in 0.1 M NaCl + 0.03 M $NaHCO_3$, and found that the corrosion products on the surface were MoO_3, $Al_2(MoO_4)_3$, $MoCl_4$, $AlCl_3$, Al_2O_3, and $Al(OH)_3$. In alkaline solutions, non-protective NiO and $Ni(OH)_2$ was reported. In all cases, addition of Mo increased the pitting potential for pure Al. Also, Bertocci [15] and Ricker [16], studied the corrosion performance of nickel aluminides in neutral, acidic and alkaline media, and found that the corrosion resistance of nickel aluminides appears to be very similar to that of pure nickel. They found that pitting of these aluminides occurred, not only in chloride-containing solutions, but also in sulfuric acid in a certain potential range.

A beneficial effect of Mo was found. However, in our case, the opposite was observed, i.e. a detrimental effect of molybdenum. For passivation to occur, the film must be adherent, non-porous and chemically inert in the solution. Pitting occurs as the dissolution of the metal at flaws and defects within the surface film when the bare metal is exposed to the aggressive anions in the electrolyte. The pitting sites are related to the metal surface conditions, such as microstructure and surface preparation, and to the electrolyte composition. To cause pitting, anions such as Cl^-, Br^-, I^-, etc. must first be adsorbed on the film surface. With anions present, pitting occurs in competition with film repair by active dissolution of the metal at flaws. To improve the pitting behavior, it must avoid the adsorption of anions and delay the breakdown of passivity. Cl^- does not affect the content of Mo in the passive layer, but Mo enhances the disorder in the passive film. Alloys containing Al are protected against corrosion by the formation of a protective Al_2O_3 layer. Incorporation of Mo into the passive film, alters the Al–O bonds and replaces them with bonds formed between oxygen and molybdenum, affecting the incorporation of aggressive anions, and therefore, affects the alloy corrosion resistance [14]. Thus, the main effect of Mo is to change the chemical properties of the surface film by altering the adsorption of ions and by affecting the corrosion dissolution resistance of the metal.

4. Conclusions

A study of the effect of Fe, Ga and Mo on the corrosion performance of NiAl in 0.5 M NaCl and 0.5 M NaOH at room temperature using electrochemical techniques was carried out. The Al–42Ni + 6Fe and Al–40Ni + 6Fe + 2-Mo alloys exhibited the best corrosion resistances in 0.5 M NaCl whereas the highest corrosion rate was for the Al–39Ni + 6Fe + 6Mo alloy. The NiAl-base alloy was the second alloy with the highest corrosion rate. In 0.5 M NaOH, the highest corrosion rate was exhibited by the Al–41Ni + 6Mo alloy, whereas the best corrosion performance was for the alloys with 6Ga, followed by the alloys containing 6Fe + 2Ga and 2Mo + 2Ga. The NiAl-base alloy had an intermediate corrosion rate value. The alloys with the lowest corrosion rate also had the lowest pitting potential value. The detrimental effect of additions of 6Mo to the NiAl alloys was explained in terms of the effect of Mo on the chemical properties of the passive film, affecting the adsorption of aggressive anions on the external layer thus breaking down the passivity.

References

1. R.D. Noebe, R.R. Bowman and M.V. Nathal, *Int. Mater. Rev.* **38** (1993) 193.
2. D.B. Miracle, *Acta Metallurgica Mater.* **41** (1993) 649.
3. R. Darolia, *J. Mater. Sci. Technol.* **10** (1993) 157.
4. E.P. George, M. Yamagochi, K.S. Kumar and C.T. Liu, *Annu. Rev. Mater. Sci.* **24** (1994) 409.
5. R.R. Bowman, A.K. Misra and S.M. Arnold, *Metall. Trans.* **26**A (1995) 615.
6. H.P. Chiu, L.M. Yang and R.A. Amato, *Mater. Sci. Eng. A* **203** (1995) 81.
7. C.T. Liu, L.M. Yang and R.A. Amato, *Mater. Sci. Eng. A* **191** (1995) 49.
8. M.S. Choudry, M. Dollar and J.A. Eastman, *Mater. Sci. Eng. A* **256** (1998) 25.
9. A. Albiter, M. Salazar, E. Bedolla, R.A.L. Drew and R. Perez, *Mater. Sci. Eng. A* **347** (2003) 154.
10. A. Albiter, E. Bedolla and R. Perez, *Mater. Sci. Eng. A* **328** (2002) 80.
11. M. Stearn and A.L. Geary, *J. Electrochem. Soc.* **105** (1958) 638.
12. P. Bruesh and K. Muller, *Appl. Phys. A* **38** (1985) 1.
13. S. Mischeler, A. Vogel, J.J. Mathieu and D. Landolt, *Corros. Sci.* **32** (1990) 925.
14. X. Zhang, S. Lo Russo, S. Zandolin, A. Miotello, E. Cattaruzza, P.L. Bonora and L. Benedetti, *Corros. Sci.* **43**(1) (2001) 85.
15. U. Bertocci, J.L. Fink, D.E. may, P.V. Madsen and R.E. Ricker, *Corros. Sci.* **31**(3) (1990) 471.
16. R.E. Ricker, *Mater. Sci. Eng. A* **198** (1995) 231.
17. R. Cortes, M. Froment, A. Hugot-Le Goff and S. Foiret, *Corros. Sci.* **31** (1990) 121.